Biochimica et Biophysica Acta 1798 (2010) 719–729

Contents lists available at ScienceDirect

Biochimica et Biophysica Acta

journal homepage: www.elsevier.com/locate/bbamem

Review

Silica xerogel/aerogel-supported lipid bilayers: Consequences of surface corrugation

Emel I. Goksu [a], Matthew I. Hoopes [a], Barbara A. Nellis [a,b], Chenyue Xing [a], Roland Faller [a], Curtis W. Frank [c], Subhash H. Risbud [a], Joe H. Satcher Jr. [b], Marjorie L. Longo [a,*]

[a] Department of Chemical Engineering & Materials Science, University of California, Davis, CA 95616, USA
[b] Chemistry, Materials, Earth and Life Sciences Directorate, Lawrence Livermore National Laboratory, 7000 East Avenue, Livermore, CA 94550, USA
[c] Department of Chemical Engineering, Stanford University, Stanford, CA 94305, USA

ARTICLE INFO

Article history:
Received 3 July 2009
Received in revised form 2 September 2009
Accepted 7 September 2009
Available online 18 September 2009

Keywords:
Atomic force microscopy
Quartz crystal microbalance
Membrane raft
Coarse-graining
Porous material
Membrane bending

ABSTRACT

The objective of this paper was to review our recent investigations of silica xerogel and aerogel-supported lipid bilayers. These systems provide a format to observe relationships between substrate curvature and supported lipid bilayer formation, lipid dynamics, and lipid mixtures phase behavior and partitioning. Sensitive surface techniques such as quartz crystal microbalance and atomic force microscopy are readily applied to these systems. To inform current and future investigations, we review the experimental literature involving the impact of curvature on lipid dynamics, lipid and phase-separated lipid domain localization, and membrane–substrate conformations and we review our molecular dynamics simulations of supported lipid bilayers with the atomistic and molecular information they provide.

Contents

1. Introduction . . . 719
2. Silica xerogels/aerogels . . . 720
3. Fluid lipid bilayers supported on aerogel and xerogel substrates . . . 722
4. Phase-separated lipid bilayer supported on xerogel substrate . . . 724
5. Experimental curvature effects in supported bilayers . . . 724
6. Molecular modeling of rough and patterned surfaces . . . 726
7. Conclusions . . . 727
Acknowledgements . . . 727
References . . . 728

1. Introduction

Supported lipid bilayers have been extensively used as model systems for cell membranes offering the possibility of applying surface sensitive techniques such as atomic force microscopy (AFM) [1-4], time-of-flight secondary ion mass spectrometry (SIMS) [5] and high resolution nanoSIMS [6,7]. The procedures for preparing solid supported lipid bilayers via Langmuir-Blodgett or vesicle fusion techniques are well established and described in the literature [1,8]. Important differences exist between free and supported lipid bilayers. In a free bilayer, static curvature (vesicles, tubules, etc.) or dynamic bending modes induced by thermal fluctuations are mediated by constituent lipid intrinsic curvature and bending and tension elasticity [9,10]. These properties are the result of hydrophobic portions of the membrane trying to minimize exposure to an aqueous solvent. However, on smooth hydrophilic surfaces, a layer of water organizes in an ice-like structure [11,12]. This structure's energetically favorable interaction with the water hydrating the polar head groups of the lipids in the membrane drives adsorption but the entropic penalty of adsorption not only limits thermal fluctuations in the membrane [13] but also modifies the natural pressure profile across the bilayer [14]. As the roughness of a support transitions to nanometer or larger corrugations, a competition between membrane tension, curvature, and adsorption energy emerges [15], while thermal fluctuations, e.g. protrusion modes are modified in relation to the local roughness [11].

* Corresponding author. Tel.: +1 530 754 6348; fax: +1 530 752 1031.
E-mail address: mllongo@ucdavis.edu (M.L. Longo).

0005-2736/$ – see front matter © 2009 Elsevier B.V. All rights reserved.
doi:10.1016/j.bbamem.2009.09.007

Motivating current studies of supported lipid bilayers on customized surfaces is the effort to utilize the convenience of a macroscopically planar and mechanically stable platform for experimentation, while creating a lipid environment more closely resembling the biological systems being modeled. Soft matter spacers between the bilayer and support [16,17] or the use of porous substrates optimally would act to both reduce adsorption constraints on supported membranes, provide solvent access to both leaflets of the bilayer [18], and allow transmembrane and membrane associated molecules such as proteins and saccharides an environment free of steric hindrances [19]. While new supports attempt to address these concerns, they also provide a new way to observe relationships between curvature, lipid organization, and phase behavior in lipid mixtures.

Lipid bilayer formation via vesicle fusion on various silica surfaces has been studied on various materials such as quartz [20], organosilane SAMs [21], nanoporous microbeads [22-24], chemically oxidized silicon [25], glass [26], colloidal crystals [27,28], nanocomposite thin films [29], and aerogels/xerogels [30,31]. Studies on the properties of porous silica thin film materials produced via sol–gel chemistry have been well documented in the literature [32-34]. Silica xerogels as supports for phospholipid bilayer formation have been studied here and are advantageous substrates for these studies because these materials have controllable surface porosity, have unique surface chemistry and can be easily produced for a variety of applications.

Cell membranes are richly heterogeneous in their composition and therefore understanding the behavior of multicomponent lipid bilayers supported on new substrates is of interest. Multicomponent, phase-separated lipid bilayers that contain gel phase domains are a logical choice for deposition onto new substrates since there is accumulated evidence for the existence and importance of local lipid ordering (lipid rafts and microdomains) in several biological processes [35,36]. In a phase-separated bilayer, the gel phase domains are more packed and extend above the more disordered phase allowing examination by height-sensitive techniques such as ellipsometry [37] and atomic force microscopy [38].

Here we review our recent investigations that combine considerations of substrate roughness and curvature with studies of bilayer behavior on these surfaces. We focus on the sol–gel process for substrate preparation due to ease of parameterization and preparation. We review two studies of lipid bilayers supported on sol–gel derived silica substrates (aerogels and xerogels). The first study employed quartz crystal microbalance with dissipation (QCM-D) and fluorescence recovery after photobleaching (FRAP) to characterize the vesicle fusion process and lipid diffusion respectively [30,31]. The second study employed atomic force microscopy (AFM), FRAP, and fluorescence correlation spectroscopy (FCS) to characterize binary phase-separating lipid mixtures on silica xerogels [39]. These studies constitute initial steps toward examining and understanding more complex biomimetic membranes on surfaces where curvature plays a significant role. We highlight literature that informs these studies with current work involving the impact of curvature on lipid organization, domain locations, and membrane–substrate conformations. Additionally, we review molecular dynamics simulations of supported lipid bilayers with the atomistic and molecular information they provide [11,14,40]. This rich area of exploration promises to provide many opportunities for further elucidation of membrane properties and behaviors.

2. Silica xerogels/aerogels

In general, the sol–gel preparation of porous materials requires three basic steps: (1) formation of a stable colloid (sol), (2) gelation and (3) drying. Wet gels of inorganic oxides are typically prepared through the hydrolysis and condensation of their alkoxides or inorganic salts (for example see Fig. 1), leading to the formation of a three dimensional network. The gelation process results in the formation of a liquid-filled solid network, and to produce a dried solid structure, the solvent that resides within the pores of the gel structure is removed. Two basic approaches can be used to dry sol–gel materials: (1) solvent evaporation, and (2) supercritical fluid processing extraction. In the case of solvent evaporation, large capillary forces are generated as the liquid meniscus migrates through the small cells and pores of the gel. These capillary forces lead to significant shrinkage (sometimes greater than 75% by volume), and precautions must be taken to prevent cracking of the gel. Once dried, the solid product, xerogel, may have a porosity of 0%–50% depending on the precursor chemistry. Porosity of a solid is generally defined as the ratio of void pore volume to the volume of the whole. The IUPAC defines micro-porosity as materials with pores smaller than 2 nm in diameter, macro-porosity materials have pores larger than 50 nm and meso-porosity includes the range between 2 and 50 nm [41]. Porous thin films can be produced by spin coating (see Fig. 2) or dip coating the sol onto a substrate. Aerogels are obtained if the solid can be dried without the collapse of the gel network (see Fig. 2).

Aerogels are a special class of open-cell foams derived from highly cross-linked inorganic or organic gels that are dried using special techniques to preserve the tenuous solid network. By definition, these materials are prepared through the sol–gel process and can be either granular or monolithic. Aerogels have ultrafine cell/pore sizes (less than 1000 Å), continuous porosity (typically >75%), high surface area (400–1000 m^2g^{-1}), and a microstructure composed of interconnected colloidal-like particles or polymeric chains with characteristic diameters of 100 Å. This microstructure is responsible for the unusual optical, acoustical, thermal, and mechanical properties of aerogels. For example, aerogels are known to exhibit the lowest thermal conductivity, sound velocity, and refractive index of any bulk solid material. In addition, aerogels can be prepared as transparent solids because their ultrafine cell/pore size minimizes light scattering within the visible spectrum. Most of the properties characteristic for bulk aerogels are also exhibited in other forms of the material, such as thin sheets or films, an important aspect for a growing number of electronic and thermal applications.

Aerogels are among the most versatile materials available for technical applications due to their wide variety of exceptional properties. Technological interest in aerogels originated from the need in high-energy physics experiments for low density materials

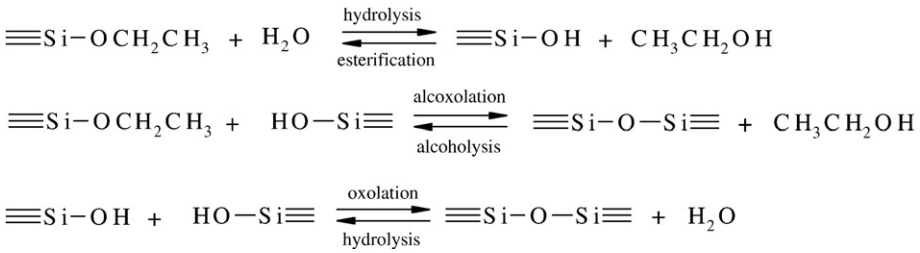

Fig. 1. Governing synthesis reactions for silica sol–gel chemistry with tetraethyloxysilane as precursor.

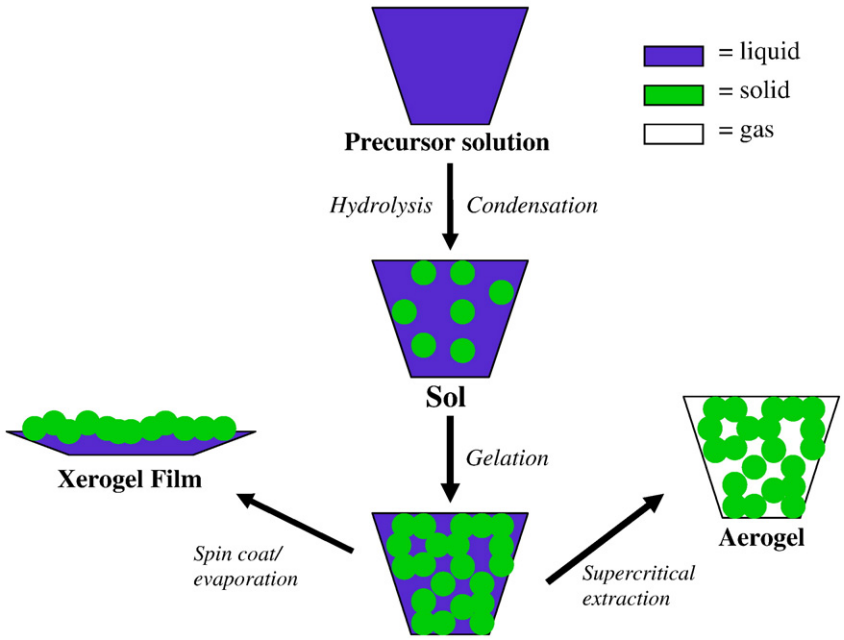

Fig. 2. General scheme for preparing aerogel and spin coated xerogel by sol–gel processing.

with good optical qualities. Due to their low index of refraction, silica aerogels were identified as good candidates for the design of Çerenkov counters used in the detection of nuclear particle radiation [42]. Since then, aerogels have been used or considered for use in laser experiments, sensors, thermal insulation, waste management, molds for molten metals, optics and light-guides, electronic devices, capacitors, high explosive research, imaging devices, catalysts, pesticides, cosmic dust collection and X-ray laser research.

In silica sol–gel synthesis, as shown in Fig. 1, a chemical precursor such as a tetraethoxysilane undergoes hydrolysis and condensation reactions forming siloxane bonds catalyzed by either an acid or base [32]. As the reactions progresses, a colloidal suspension of silica beads

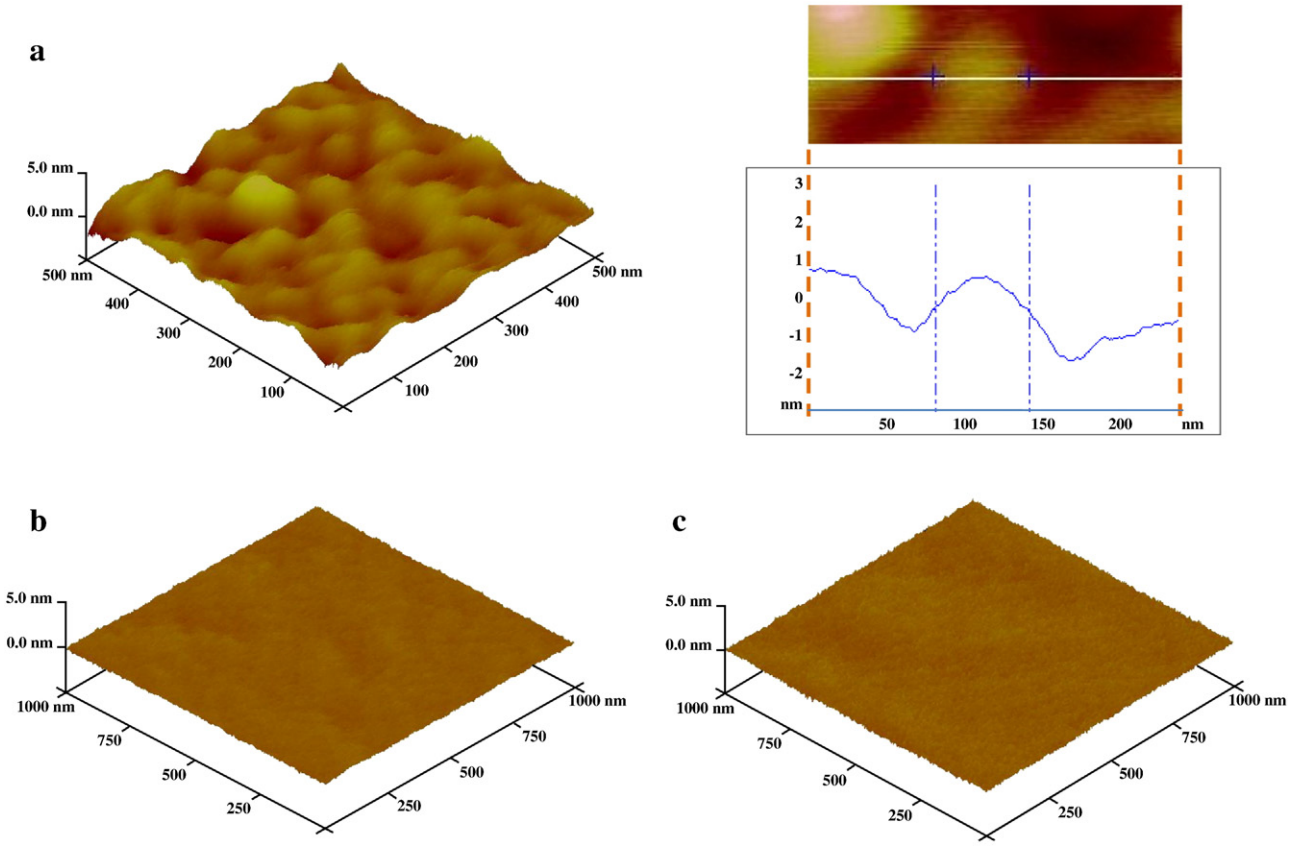

Fig. 3. Atomic force microscope image(s) of (a) silica xerogel surface prepared as described in Section 4 (a typical ~50 nm surface feature is demonstrated in the cross-section), (b) quartz surface (SPI Supplies, number zero quartz coverslip), and (c) borosilicate glass surface (Fisherbrand, number one microscope cover glass).

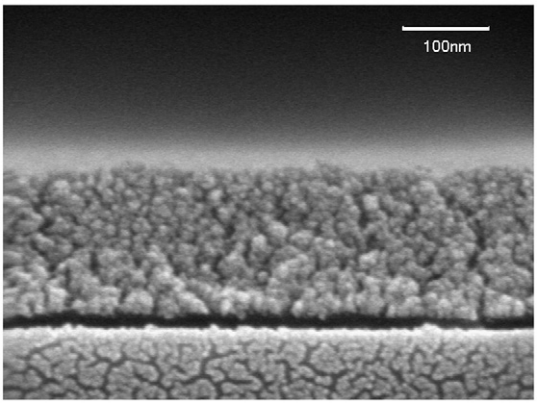

Fig. 4. Scanning electron micrograph of silica xerogel cross-section.

form, then finally gel to create a continuous liquid phase surrounding a silica bead network which spans the reaction container. Xerogels are produced by allowing the solvent to evaporate during which the capillary forces collapse the skeletal structure resulting in a decrease in bulk porosity. Aerogels are produced when a supercritical extraction of the liquid phase, generally alcohol or carbon dioxide, is performed thereby preserving the continuous solid network of nanoparticles without appreciable shrinkage of the solid framework. The porosity of silica aerogels can be up to 99.8% whereas the porosity of a xerogel can range from 0% to 50% [43]. The reaction kinetics, synthesis parameters, and structure of the resulting gels have been extensively studied in the literature [44-48]. In general, the gelation time is controlled by altering the amounts of the reactants and the casting method used; i.e. spin coating, dip coating, bulk gelation, etc. The porosity, pore size, and gel structure can be controlled by the type and amount of catalyst used. Acid-catalyzed silica sol–gel reactions result in a randomly branched, linear structured gel whereas base-catalyzed reactions produce highly branched cluster structures [32].

Silica aerogels and xerogels are useful in many applications. As supports for phospholipid bilayers, silica xerogels have a great deal of potential given the ease of synthesis and the ability of the liquid to conform to different shapes prior to gel formation and the robust behavior of the gel in aqueous solutions [39]. The surface features of a typical silica xerogel compared to quartz and borosilicate glass surfaces are shown in Figs. 3 and 4. Silica xerogel surfaces are uniquely compatible as scaffolds for vesicle fusion and bilayer formation as a result of some desirable properties, primarily their hydrophilic nature and controllable surface pore size.

3. Fluid lipid bilayers supported on aerogel and xerogel substrates

Silica aerogels and xerogels created via the sol–gel synthesis method were used as substrates for phospholipid bilayers formed via vesicle fusion [30,31]. In these works, small unilamellar egg phosphatidylcholine (PC) vesicles in solution were used to form bilayers on a variety of surfaces including silica xerogel and silica aerogel (Fig. 5), Vycor® glass, silicon oxide and borosilicate glass. Vycor® glass is a registered trademark of Corning Incorporated and has been characterized to have a monodispersed pore size centered around 60 Å with a porosity of ~28%. Vycor® glass has a grain sizes ranging from ~0.3 to 4 μm with a silica bead plate-like structure [30]. In one study [30], fluid bilayers on xerogel, aerogel, and silicon oxide were observed and compared using quartz crystal microbalance with dissipation (QCM-D), epifluorescence microscopy and fluorescence recovery after photobleaching (FRAP); the substrates were characterized using scanning electron microscopy (SEM). Another study [31] focused on lipid diffusion behavior via FRAP on mesoporous silica xerogels, aerogels, Vycor® glass and borosilicate glass and the impact of cracks in the substrate to confine fluorescence recovery after photobleaching. Collectively, these studies represent a coherent initial survey for these mesoporous, sol–gel synthesized, silica materials as supports for lipid bilayers formed through vesicle fusion.

Typical surface features of the substrates were 10–25 nm diameter beads for silica aerogel and 36–104 nm beads for silica xerogel. The pores in these materials were 10–25 nm in scale for aerogel and 9–24 nm for xerogel from SEM micrographs. Vycor® glass has monodispered pores of 6 nm and a porosity of ~28%. Silica aerogels and xerogels investigated have porosities ranging from ~75% to 99.8% and ~0%–52%, respectively. The borosilicate glass, on the other hand, has zero porosity and is considered to be relatively smooth compared to the others [49].

To understand the underlying interactions which govern vesicle fusion and bilayer formation on these tortuous materials, QCM-D data were analyzed and interpreted for a silica xerogel thin film and compared to thermally evaporated silicon oxide. In QCM-D, adsorption and transformation of vesicles are observed by measuring the frequency change and dissipation energy change of a quartz crystal. For example, an increase in mass of a soft film, such as a bilayer, would result in a decrease in the crystal's resonance frequency as well as an increase in the dissipation energy due to the soft nature of the material [50]. The results from the QCM-D data show that the lipid bilayer forms on the silicon oxide surface nearly four times faster than on the silica xerogel film [30]. It was also found that the resonance frequency change as well as the absolute change in dissipation energy for the formed bilayer was greater for silica xerogel than that for the silicon oxide indicating that ~10% more bilayer material was adsorbed onto the xerogel support [30]. It was reported that this value was likely to be an underestimation of the actual mass due to neglect of the viscoelastic component of the intact vesicles.

In discussion of these results, it is speculated that the large surface area and roughness of the xerogel support may actually create a bottleneck step in the bilayer formation during the vesicle fusion process. The uneven surface may have reduced surface–vesicle interactions compared to a smooth silica surface where all hydrophilic surface silanol groups appear in the same plane. An increased surface area would require a larger amount of vesicles for the critical coverage to promote coalescence and the rough terrain of the surface may also hinder the spreading of the bilayer during the intermediate steps of vesicle fusion. As vesicle fusion occurs, an increased amount of surface area would account for the additional mass of bilayer material on the silica xerogel surface if the bilayers conformed to the corrugated surface to some degree (as depicted in Fig. 5).

The lateral mobility of lipids on these surfaces was studied by FRAP technique and the results were compared. The bulk compositions of

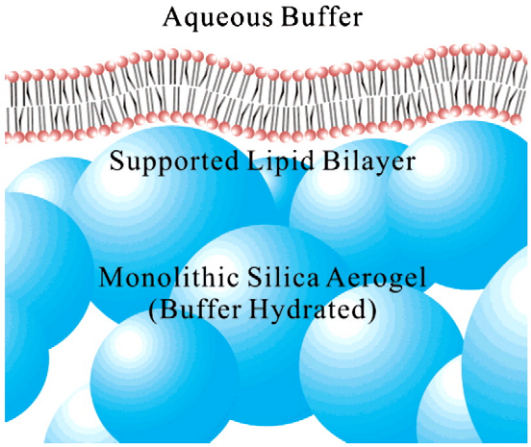

Fig. 5. A schematic representation of an aerogel-supported lipid bilayer. The topology and the sizes of the lipids and the beads are not based on experimental observations. Reprinted with permission from [30]. Copyright 2004 American Chemical Society.

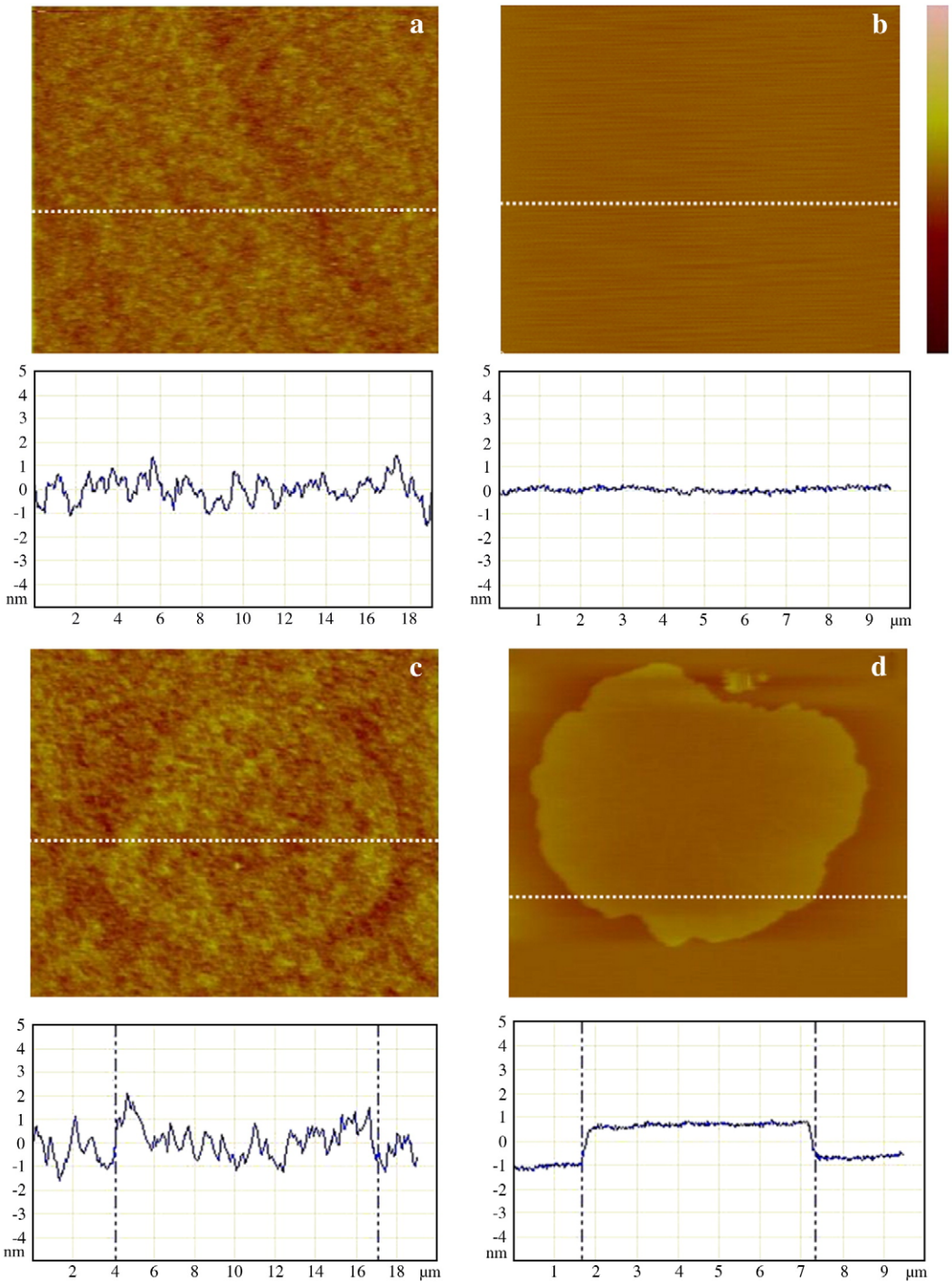

Fig. 6. AFM images and section analysis of (a) bare silica xerogel surface, (b) bare mica surface, (c) DOPC-DSPC bilayer on silica xerogel, and (d) DOPC-DSPC bilayer on mica. (a, c) 15.5 μm × 19 μm, (b, d) 8.3 μm × 9.5 μm. The dotted lines in the AFM images indicate the location of the sections and the dotted lines in the sections in panels c and d indicate the edges of DSPC domains. The color scale bar on the right represents 15 nm. Reprinted with permission from [39]. Copyright 2009 American Chemical Society.

the substrates that were used in this study are not significantly different from each other; therefore, any difference in the diffusion results was expected to be due to the morphology of the surface rather than the surface chemistry. The diffusion coefficients of lipid in bilayers on silica aerogel, xerogel, Vycor® glass and borosilicate glass were measured to be 0.6 ± 0.2, 2 ± 1, 1.7 ± 1.1 and 2.5 ± 0.4 $\mu m^2/s$, respectively; approximately, with an increasing trend as the surface corrugations and porosity decreased [31]. Mobile fractions of the lipids also more or less follow this trend, i.e. 75%, 81%, 94% and 100%, respectively [31]. This behavior was qualitatively attributed to the bilayer following the surface contours of the highly undulating substrates to some extent and also to the sensitivity of the bilayer to the defects on the surface. These two points will be addressed quantitatively in Section 4.

The aerogel structures can undergo partial collapse due to the induced capillary forces upon fluid absorption. Accordingly, fluorescence images revealed the presence of deep and irregular cracks on the surface of the aerogel-supported bilayers. Similarly, in the xerogel thin films, the surface could be observed to be in several different geometric forms; some regions appeared defect-free and others

contained extensive cracking. At this point, one may consider the possibility that the bilayer spans across those micron-size cracks. To address this issue, the xerogel surfaces where cracks were present were further examined and it was observed that the lipids did not uniformly redistribute after photobleaching indicating that the cracks served as barriers of lateral motion and divided regions of supported membranes [31].

Overall, these studies demonstrated that fluid phase lipid bilayers could be successfully prepared on nanoporous silica supports and that surface corrugation can slow supported lipid bilayer formation kinetics and lipid diffusion.

4. Phase-separated lipid bilayer supported on xerogel substrate

Several studies directed at the cell membrane have provided evidence for the existence of lipid and protein heterogeneities in the submicron range which are integrally involved with various cell functions such as trafficking of proteins and lipids [51], cell signaling [52], and protein sorting [53]. A model membrane of heterogeneous lipid composition (and concomitant heterogeneous ordering) can be easily formed through lipid phase separation and provides a compositionally flexible and relatively easily characterized system. Therefore, the study of aerogel/xerogel-supported fluid lipid bilayers [30,54], summarized in the previous section, was followed by introduction of gel phase domains into the lipid bilayers via lipid phase separation of a binary lipid bilayer [39]. The presence of the gel phase domains also provided a frame of reference in AFM and fluorescence imaging to distinguish xerogel-supported lipid bilayer from xerogel and estimate the actual bilayer area (vs. projected area) on a xerogel vs. mica support respectively.

Silica xerogel structures were prepared, each under identical experimental conditions (one-step base-catalyzed sol–gel synthesis using tetramethoxysilane as the precursor and spin coated onto freshly cleaved mica substrates at 10 min of the gelation process) and characterized by using AFM (Fig. 6a). By examining cross-sections of 1 μm × 1 μm images (see Fig. 3a), xerogels prepared in this way were found to have a feature size of 50 ± 21 nm that each appears to be a colloidal-like bead (see Fig. 3a) [39].

When a 2:1 dioleoylphosphatidylcholine (DOPC)–distearolylphosphatidylcholine (DSPC) vesicle solution was deposited on the silica xerogel surfaces and cooled from 65 °C to room temperature, successful vesicle fusion and fluid-gel phase separation were observed by AFM as shown in Fig. 6c where a DSPC-rich domain is readily visible [39]. The surface roughness of the lipid bilayer on silica xerogel was quite similar to the surface roughness of the silica xerogel (compare Fig. 6a and c) indicating that the bilayer followed the silica xerogel surface closely rather than being suspended on the substrate under contact mode AFM imaging conditions. The average RMS roughness values for silica xerogel and silica xerogel-supported lipid bilayers obtained from 20 μm × 20 μm images were 0.71 ± 0.28 nm and 0.59 ± 0.04 nm, respectively, which were not significantly different from each other by *t*-test. Mica seen in Fig. 6b and mica supported bilayers seen in Fig. 6d were smoother having RMS roughness values of 0.12 ± 0.02 nm and 0.07 ± 0.01 nm, from contact mode AFM respectively.

To quantify the degree of corrugation imposed upon the lipid bilayer by the xerogel support, the actual amount of lipid bilayer area was compared to the projected area by quantitative fluorescence. AFM was not used for this measurement because the tip cannot penetrate into the porous xerogel material and therefore such a measurement by AFM on a nanoporous material will be greatly in error. A comparison was made of the NBD-PC fluorescence intensity difference between the surrounding DOPC-rich fluid phase and symmetrically distributed (spanning both leaflets) DSPC-rich domains on mica vs. silica xerogel. The intensity difference between DSPC-rich symmetric domains and the surrounding DOPC-rich fluid phase was found to be 1.96 ± 0.26 times higher for the bilayer on the silica xerogel side compared to DSPC-rich domains on the mica side of the same substrate [39]. In other words, the real bilayer area was doubled on xerogel compared to mica. A plausible explanation for this result is that the lipid bilayer follows the surface contours covering approximately half of each silica bead on the surface.

In agreement with the real areas, the lipid diffusion coefficient in DOPC bilayers was significantly slower, 1.69 ± 0.53 $\mu m^2/s$, on silica xerogel support compared to a mica support, 3.93 ± 0.98 $\mu m^2/s$, as calculated by FRAP at room temperature [39]. The fluorescence in the FRAP spot was recovered almost completely (>95%) as the measurements were done on micron-scale defect free regions and the substrates were pre-bleached before bilayer formation. Increasing the area by 1.96 times in the FRAP equations used for calculating the diffusion coefficient on silica xerogels accordingly resulted in a value of 3.31 ± 1.05 $\mu m^2/s$ which is not statistically different from the diffusion coefficient on mica (3.93 ± 0.98 $\mu m^2/s$) [39]. The agreement between diffusion coefficient and membrane area gives credence to the idea that there is significant coverage of the silica beads by the lipid bilayer and the basic reason underlying the reduced diffusion coefficient is the bilayer following the surface curvature of each surface-exposed ~50 nm bead.

Moreover, the diffusion coefficients obtained for both mica and silica xerogel-supported bilayers by fluorescence correlation spectroscopy (FCS) technique (1.65 ± 0.26 and 4.31 ± 0.13 $\mu m^2/s$, respectively) were observed to be similar to the FRAP results [39]. Since the defects within the bilayer would be more pronounced in the larger FRAP spot as compared to the FCS spot, the FCS results are expected to be higher if there are defects present within the bilayer [55]. Therefore, these similar results using FCS and FRAP can be interpreted to indicate negligible defect formation in silica xerogel (and mica) supported bilayers which is in agreement with the results of Roiter et al. [56], discussed in the next section, stating that continuous bilayer formation can be achieved on the nanoparticles having diameters larger than 22 nm.

DSPC-rich domain density and size on the silica xerogel compared to mica supports were analyzed by using fluorescent images. The domain area per projected area (or real area) ratio was higher on silica xerogel (0.224 vs. 0.176) [39]. In addition, the domain number per real area on the silica xerogel substrate was approximately half (18 domains / $(100\ \mu m)^2$) of that on the mica substrate [39]. These findings indicate that there is a significant difference in the thermodynamics of a supported bilayer that conforms to a corrugated surface with surface radii in the 25 nm scale vs. a flat (0.1 nm roughness) surface. We will review the literature in this area in order to gain a better understanding of the thermodynamics of lipid bilayers conforming to curved surfaces in the next section.

5. Experimental curvature effects in supported bilayers

At least three distinct issues exist when discussing the effect of curvature on supported lipid bilayers. First, there is the question of what individual lipids do in a curved environment. Lipids have curvature preferences depending on their shape. This intrinsic curvature preference can lead to many different phases in three dimensional lipid structures [57]. Second, there is the question of what phase-separated domains do in laterally segregated lipid mixtures when interacting with curvature in the membrane. In addition to the individual preferences of lipid molecules, membranes in different phases will have varying mechanical properties that mediate their behavior [58]. Third, there is the broad question of how a supported lipid bilayer interacts with a corrugated surface that would initially induce curvature in the membrane. This too depends on membrane properties such as edge energies around defects and the bending stiffness of the membrane as well as the chemical properties of the surface and the adhesion it induces [59].

Fig. 7 shows a sample of studies that investigate curvature and concomitant support features with the ranges of radii of curvature inferred.

Addressing the first question, the recent work by Tian and Baumgart [60] has shown the absence of effective lipid sorting by membrane curvature in membranes using a single lipid species (POPC) with tracer dyes. This work looked for the preference of a lipid analogue dye to locate to either the relatively low curved membrane area of a giant unilamellar vesicle (GUV) or the highly curved area of a microtubule-like tether extended from the GUV. Curvature on the microtubule was as high as 0.1 nm^{-1} (a radius of 0.01 μm) while a representative GUV provided a curvature of 0.1 μm^{-1} (a radius of 10 μm). Lipid analogue dyes with two different head-group-attached fluorophores (Texas Red (TR)-DHPE and BODIPY-DHPE) as well as ones with three different tail groups (DiI-C_{18}, DiI-C_{12}, and Fast DiI) did not preferentially change concentrations as a result of changes of curvature between the relatively low curvature of a GUV and the high curvature of an extended tubular tether. On the other hand fluorescence measures of the localization of Cholera Toxin B, which binds clusters of five ganglioside lipid (M1) GM1 species that were added to the membrane at low concentrations, showed that GM1 sorted to areas of low curvature.

With the evidence above that individual lipids do not appear to be curvature sorted, one can ask what effect curvature has on the mobility of lipids. In experiments where membranes were formed on colloidal crystals, Brozell et al. [27] showed that the diffusion measured by FRAP showed that recovery was 4–6 times slower when using 330 nm silica beads for the colloidal crystals compared with supported lipid bilayers on a glass coverslip but it was suggested that this was accounted for by considering the three dimensional path of the lipids rather than using the distances in the projected image plane. Sanii et al. [61] also looked at diffusion on corrugated surfaces with curvatures from 0.01 to 0.13 μm^{-1} where the patterned surface was made by rows of wrinkles in PDMS. FRAP measurements showed the Gaussian profile of the bleached spot change to an ellipse that was oriented with the two axes of the corrugation, parallel and perpendicular to the wrinkles. A more rigorous study by Werner et al. [62] found that membranes that closely conformed to a corrugated surface show anisotropic FRAP recovery which was quantitatively explained by the additional path length lipids traveled when moving perpendicular to the one dimensionally patterned corrugations of the surface. These results indicate that curvature at these levels do not change the diffusion rates of lipids.

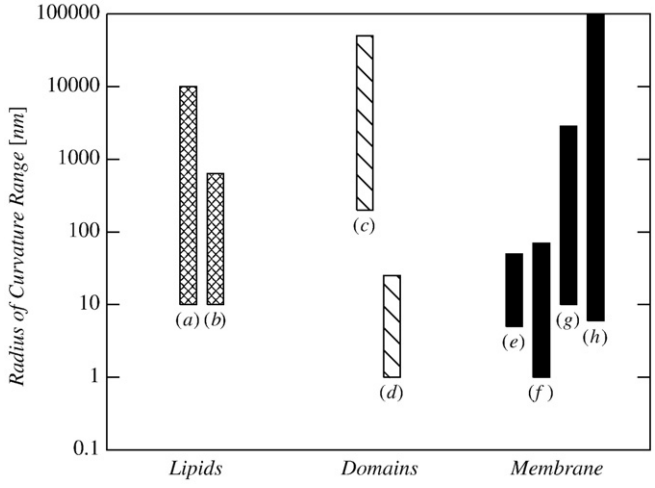

Fig. 7. A summary of curvature radii addressed in selected references. Some references state explicit curvatures and others are inferred from descriptions of substrate features. (a) Tian [60] (b) Werner [62] (c) Parthasarathy [63] (d) Goksu [39] (e) Davis [24] (f) Roiter [56] (g) Brozell [27] (h) Sanii [61].

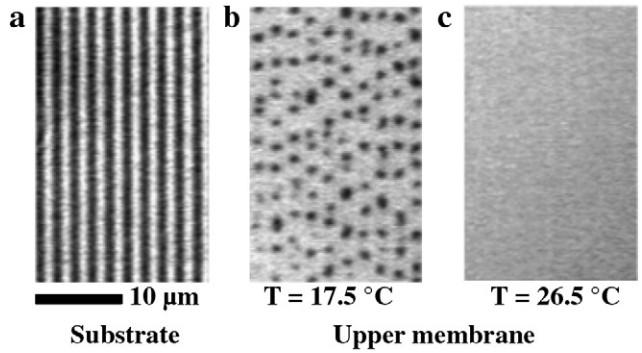

Fig. 8. Curvature effect on domain location. (a) Brightfield image of the substrate. (b) In a mixture of DOPC/DPPC/cholesterol/DOTAP/TR-DPPE (of mol% 52.9/15.1/30/1.5/0.5), dark predominantly DPPC-rich L_o lipid domains align with lower curvature regions of the membrane. (c) Lipids mixed at higher temperature. Reprinted with permission from [63]. Copyright 2006 American Chemical Society.

Since lipids appear to not necessarily be curvature sorted as individual molecules, the second question of phase-separated domains is important to address since one might ask if curvature can induce phase changes or if domains preferentially grow in curvature directed regions. Parthasarathy et al. [63] observed curvature dependent partitioning between phases in a ternary mixture of DOPC, DPPC, and cholesterol where the L_o domains preferentially grow in areas of low curvature. Fig. 8 shows images of the substrate and the transition from miscibility to L_o domain formation. It was found that a critical minimum curvature of 0.8 μm^{-1} exists above which spatial organization of lipids occurs. This study also indicated that the difference in bending elasticity in L_o and L_d at the chosen cholesterol concentration of 30 mol% is about 10%. Note that the authors [63] used a double-supported lipid bilayer to prevent the domains from being "pinned" to the substrate. This double bilayer was formed by vesicle fusion followed by rupture of a GUV composed of the ternary mixture. All other supported lipid bilayers discussed in this review were comprised of a single lipid bilayer formed using vesicle fusion. For details about the mechanism of vesicle fusion, the reader is directed to a recent review [38].

There is a distinct possibility that cholesterol is curvature sorted. Cholesterol is known to move spontaneously between vesicles, having a rate decreasing as the size of the donor vesicle is increasing with no significant effect of the acceptor vesicle [64]. This could be ascribed to the increased hydration of cholesterol molecules and decreased phospholipid–cholesterol interactions as a consequence of the larger area per molecule due to the higher curvature [64]. In another work, in which monolayers of binary mixtures of brominated di18:0PC and cholesterol was studied, cholesterol was also observed to accumulate in high curvature regions in distorted hexagonal phases whereas no obvious sorting was observed in lamellar or hexagonal phases [65].

In studies related to the third question, recently, it was shown that surface curvature can yield the loss of integrity and pore formation within the bilayer. L-α-Dimyristoyl phosphatidylcholine (DMPC) bilayers fused from vesicles onto silicon wafers decorated with 1–140 nm size silica nanoparticles exhibited nanoparticle-scale pores centered at 1.2–22 nm nanoparticles [56]. However, the DMPC bilayer closely followed or enveloped the surface corrugations out of that range as shown in Fig. 9. The inability to follow the surface features was attributed to the high bending penalty paid by the bilayer as opposed to the attractive force pulling the membrane to the surface [56]. In a study, in which bilayers were formed on nanoporous microbeads, it was observed that the lipid bilayers spanned pores with sizes smaller than twice the bilayer thickness. On the other hand, lipid bilayers penetrated into pores that were much larger than the bilayer thickness resulting in an increase in the membrane surface area [24].

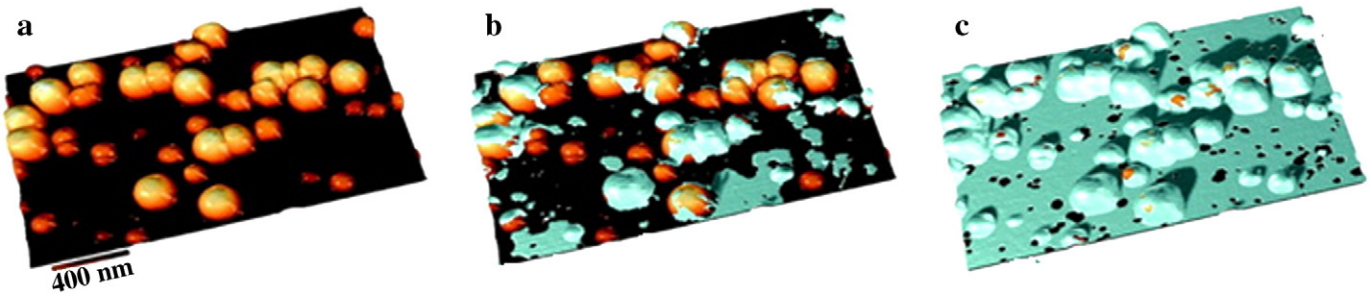

Fig. 9. Lipid bilayer formation by vesicle fusion on 5–140 nm silica nanoparticles. A series of AFM images were taken on the same location without the lipid and after the bilayers were formed. Successive AFM 3D matrices were precisely aligned and then subtracted to reveal the topology of the bilayer. (a) Substrate with nanoparticles and no lipid bilayer, (b) partial coverage of the surface by lipid bilayer, and (c) lipid bilayer formed on the surface. The bilayer covers larger particles almost completely, but holes remained around smaller particles. Adapted with permission from [56]. Copyright American Chemical Society 2008.

Recent research illustrated that curvature can also induce internal structural changes within the biomembranes [66]. It was previously reported that the outer and the inner leaflets of small unilamellar vesicles exhibited different lipid packing because of the differences in the curvature [67]. Furthermore, the phase transition temperatures of lipids with various chain lengths supported by 4–5 nm silica beads on heating (T_m) and cooling (T_c) were observed to exceed the T_m/T_c of the parent multilamellar vesicles suggesting that an interdigitated state of the lipids was favored due to high curvature and increased spacing between head groups [66].

6. Molecular modeling of rough and patterned surfaces

Molecular modeling allows unrivaled resolution through access to all particle position and velocities at all times [68, 69]. Therefore it is an ideal technique to address questions of biomembranes on surfaces and elucidate the influence of surface patterning, corrugation, or roughness [11,40,70]. There are a variety of length scales which are important in the interaction between membranes and surfaces. Therefore there is no single model which can be applied to this complex problem. It is necessary to resort to modeling on different scales.

The computational investigation of supported bilayers is a relatively new field and the relevant interactions are largely on the intermediate to large length scale. A few atom-based simulations of supported bilayers have appeared [70-74] but generally coarse grained models for lipids are a good starting point to study supported bilayers [11,40]. The solid supports in experiments are never perfectly smooth. Recently a significant amount of research has focused on topologically patterned surfaces [27,61-63]. We give here a brief overview of simulations of membranes on non-flat surfaces. We do not discuss simulations of supported bilayers in general as this has been reviewed in detail recently [70,75]. Simulations have the advantage that the roughness can be perfectly controlled and thus one can study different implementations of roughness.

Molecular dynamic simulations of lipid bilayers improve on the treatment of biological membranes with analytical elastic theory in two ways. First, when the complexity of the curvature increases, shape equations and bending Hamiltonians quickly become difficult to solve analytically, whereas MD energy calculations are computed with equal ease for any configuration. Second, in reality, lipids need not align their major axis parallel to the radius of curvature, which might lead to conformations of lower than expected energy in regions of high curvature. Typical treatment with elastic theory would not account for the resulting bending elasticity heterogeneities in such cases. Since MD is particle based, these conformations can naturally occur and are accommodated in energy calculations.

Our current work on supported lipid bilayers adds to the past work where corrugations are of atomic or molecular scale [11,40]. Previously it was shown that with controlled surface energy density, variations in corrugations of one nanometer or less do not significantly change the equilibrium structure of the membrane [36].

Using a variant [11] of the well-known Martini model [76,77] it has been determined that the surface topology of a solid substrate can have significant influence on the structural and dynamic properties of the lipid bilayer. As an example differently patterned surfaces were constructed and model bilayers of DPPC molecules were floated atop

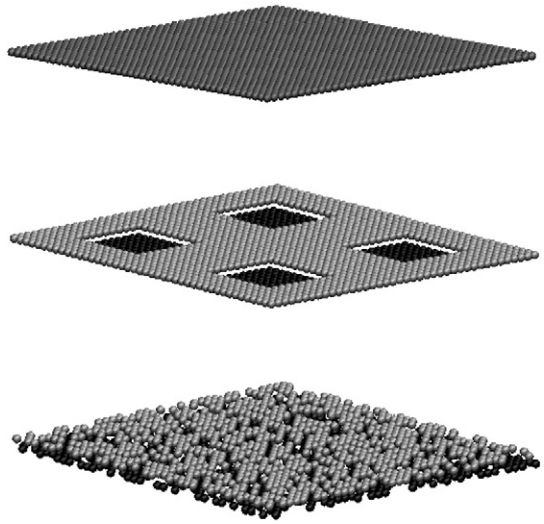

Fig. 10. Different surface topologies of solid support. From top, flat surface, dipped surface, rough surface. Adapted with permission from [11]. Copyright 2008 American Chemical Society.

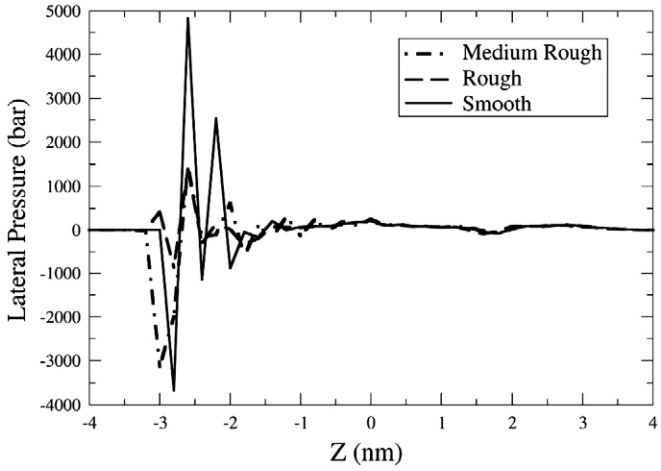

Fig. 11. Differences in lateral pressure profiles for differently rough surfaces.

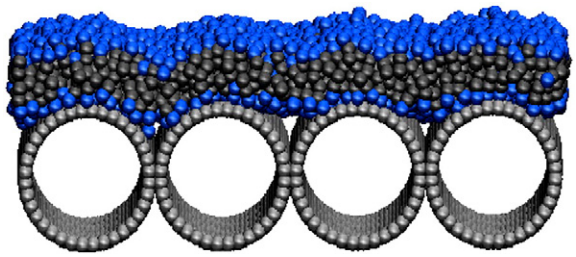

Fig. 12. Snapshot of a simulation of a water-free bilayer on a corrugated model surface.

[11]. Supported bilayer systems on a molecularly smooth, a dipped, and a randomly rough surface were studied (see Fig. 10, top, middle bottom respectively). The smooth surface is perfectly crystalline on a simple cubic lattice and all particles are in the same plane. For the dipped surface 1/4 of the total surface area is made of particles which are 0.3 nm lower than the rest, in the xy plane a simple cubic lattice is again implemented. The particles in the lower plane were grouped into 4 squares so that the surface has 4 big dips. The rough surface is again perfectly simple cubic in xy but particles are randomly assigned into two z-planes 0.3 nm apart. The lateral spacing of the surface particles on all three surfaces is 0.3 nm to ensure no solvent particles (one solvent particle represents 4 water molecules in this model) can pass through.

It turns out that the structure of the bilayers on different surfaces is significantly influenced by roughness. A typical property which is often studied is the density profile which elucidates atom positions normal to the surface. The degree of periodic ordering of the density of water and lipids was found to decrease as the roughness of the surface increases. On the smooth surface, the head groups in the proximal (closer to the support) leaflet are found in two clearly ordered layers [11]. Less pronounced layers farther from the surface can be observed with shallow patterned depressions where lateral feature sizes are much larger than a single lipid (see Fig. 10 middle surface). A more significant disordering can be seen on the rough surface. The proximal leaflet becomes similar to the distal leaflet. In addition, the mobility of lipids is also influenced by topology. With the increase in sub-molecular scale roughness and concomitant decrease in order, the lipids became more mobile. Another significant difference between various surface roughnesses is shown in Fig. 11. Here lateral pressure profiles of differently rough surfaces are shown. There is clearly qualitative agreement between different roughnesses but significant quantitative differences. The rougher a surface the smoother a pressure profile is found. This again shows that a perfectly flat surface imposes the strongest surface-induced artifacts onto a bilayer. These simulations clearly suggest that some degree of surface roughness should always be aspired to in order to minimize artifacts.

There is no symmetry plane in a supported system and there is a substantial difference in the structure of the two leaflets. There is significant localization of both, head groups and tails and increased ordering in the proximal leaflet and much less in the distal leaflet. Especially the proximal head group is highly localized and one finds a strong interaction with the support. This was also found using the water-free model by Cooke et al. [40,78]. One can find an almost crystalline behavior perpendicular to the surface in the density profile. It appears that the proximal leaflet is significantly altered whereas the distal leaflet is essentially unaffected.

If one studies supported bilayers with a water-free model one finds again that the leaflet symmetry is severely disrupted by the solid surface [40,70]. The overall thickness of the bilayer does not change substantially when considering the head group distance across the membrane. There are however, two strong effects: First the density peaks in the supported system are in general sharper and become even sharper with closer approach to the support. Second, the profile shapes are asymmetric, especially the head group peak in the proximal leaflet looks as if it has been cut in half, with a very sharp flank facing the support and a much softer slope towards the membrane center. If this model is now used to study membranes on curved surfaces it is seen that the membrane follows the rough features of the surface but not all details [Hoopes and Faller (Fig. 12 unpublished)].

This water-free model shows that membranes adsorb to surfaces with corrugations on the order of several nanometers and significantly desorb when interactions energies with the surface are half of the cohesion energy between lipids. At 10% of the cohesion energy, the bilayer is nearly returned to a planar configuration. Even lower adsorption energies allow suppressed undulation to return and macroscopic contact with the surface is no longer guaranteed. Further work is needed on corrugation scales of tens of nanometers when it becomes important to compare results with experimentally observed surface structures.

7. Conclusions

Silica xerogels and aerogels constitute a supported lipid bilayer substrate with the potential for high porosity, flexibility in substrate shape, and high local curvature. We reviewed here our experimental work showing that single component and binary (phase-separated) lipid bilayers closely follow the local corrugations (~25 nm in diameter) on the surface of the silica bead network and maintain fast fluid lipid diffusion coefficients when the real area of the bilayer is taken into account (vs. projected area). On the scale of microns, these lipid bilayers are defect free, however over larger scales, the substrate contains cracks that present themselves as obstacles for diffusion. Depending upon the intended use, these large-scale substrate defects and the longer time taken for supported bilayer formation, in comparison to flat silica, should be considered. To put this work and future experiments involving more complex multicomponent bilayers into perspective, we reviewed closely related experimental literature. Of the several studies that have been conducted on hydrophilic surfaces, all have found that membranes formed by vesicle fusion, as here, follow the local curvature of the surface closely and fluid lipids maintain their high diffusion coefficients, when real area is taken into account. The exception has been found for surfaces with smaller features (local curvature, pores), in the 1 nm–10 nm range, where bilayers are not found to simply follow the curvature of the surface. Future experiments involving xerogels/aerogels and similar corrugated substrates will involve multiple lipid and protein components. In the most closely related literature, individual lipids are not curvature sorted, however cholesterol and larger clusters of lipids and L_o domains may be partitioned or sorted according to curvature. Our recent computer simulations have focused on studying the structure and interactions of supported lipid bilayers on supports with smaller feature sizes. In agreement with these few literature studies, it is found that nanometer-scale features/roughness greatly impacts lipid bilayer structure and interaction with the substrate when compared to completely flat substrates. Overall it can be seen that trends are beginning to emerge from the works reviewed here. However it is clear that studies of supported lipid bilayers on patterned, curved and rough surfaces are in their infancy and many more studies are needed.

Acknowledgements

We acknowledge funding by the NSF NIRT Program (CBET 0506602) and the NSF MRSEC Program CPIMA (NSF DMR 0213618). M.I.H. acknowledges support by an industry/campus supported fellowship under the Training Program in Biomolecular Technology No. T32-GM08799 at the University of California, Davis. This work was partially performed under the auspices of the U.S. Department of Energy by Lawrence Livermore National Laboratory in part under

Contract W-7405-Eng-48 and in part under Contract DE-AC52-07NA27344. Some of the computer simulations were performed at the National Institute for Computational Sciences (allocation MCB070076N).

References

[1] M.-P. Mingeot-Leclercq, M. Deleu, R. Brasseur, Y.F. Dufrene, Atomic force microscopy of supported lipid bilayers, Nature Protocols 3 (2008) 1654–1659.
[2] R.P. Richter, A. Brisson, Characterization of lipid bilayers and protein assemblies supported on rough surfaces by atomic force microscopy, Langmuir 19 (2003) 1632–1640.
[3] T.V. Ratto, M.L. Longo, Obstructed diffusion in phase-separated supported lipid bilayers: A combined atomic force microscopy and fluorescence recovery after photobleaching approach, Biophys. J. 83 (2002) 3380–3392.
[4] W.C. Lin, C.D. Blanchette, T.V. Ratto, M.L. Longo, Lipid asymmetry in DLPC/DSPC-supported lipid bilayers: A combined AFM and fluorescence microscopy study, Biophys. J. 90 (2006) 228–237.
[5] N. Bourdos, F. Kollmer, A. Benninghoven, M. Ross, M. Sieber, H.J. Galla, Analysis of lung surfactant model systems with time-of-flight secondary ion mass spectrometry, Biophys. J. 79 (2000) 357–369.
[6] M.L. Kraft, P.K. Weber, M.L. Longo, I.D. Hutcheon, S.G. Boxer, Phase separation of lipid membranes analyzed with high-resolution secondary ion mass spectrometry, Science 313 (2006) 1948–1951.
[7] Y.H.M. Chan, S.G. Boxer, Model membrane systems and their applications, Curr. Opin. Chem. Biol. 11 (2007) 581–587.
[8] E.T. Castellana, P.S. Cremer, Solid supported lipid bilayers: From biophysical studies to sensor design, Surf. Sci. Rep. 61 (2006) 429–444.
[9] W. Helfrich, Elastic properties of lipid bilayers: theory and possible experiments, Z. Nat. Forsch. C J. Biosci. 28 (1973) 693–703.
[10] U. Seifert, Configurations of fluid membranes and vesicles, Adv. Phys. 46 (1997) 13–137.
[11] C. Xing, R. Faller, Interactions of lipid bilayers with supports: A coarse-grained molecular simulation study, J. Phys. Chem. B 112 (2008) 7086–7094.
[12] J. Israelachvili, Intermolecular and Surface Forces, 2nd ed.Academic Press, New York, 1991.
[13] M.C. Rheinstadter, W. Haussler, T. Salditt, Dispersion relation of lipid membrane shape fluctuations by neutron spin-echo spectrometry, Phys. Rev. Lett. 97 (2006) 4.
[14] C. Xing, O.H.S. Ollila, I. Vattulainen, R. Faller, Asymmetric nature of lateral pressure profiles in supported lipid membranes and its implications for membrane protein functions, Soft Matter 5 (2009) 3158–3161.
[15] L.D. Landau, E.M. Lifshitz, Theory of Elasticity, Pergamon Press, Inc., New York, 1970.
[16] E. Sackmann, Supported membranes: Scientific and practical applications, Science 271 (1996) 43–48.
[17] W. Knoll, C.W. Frank, C. Heibel, R. Naumann, A. Offenhäusser, J. Rühe, E.K. Schmidt, W.W. Shen, A. Sinner, Functional tethered lipid bilayers, Rev. Mol. Biotechnol. 74 (2000) 137–158.
[18] C. Danelon, J.-B. Perez, C. Santschi, J. Brugger, H. Vogel, Cell membranes suspended across nanoaperture arrays, Langmuir 22 (2006) 22–25.
[19] P.V. Ganesan, S.G. Boxer, A membrane interferometer, Proc. Natl. Acad. Sci. 106 (2009) 5627–5632.
[20] J. Xu, M.J. Stevens, T.A. Oleson, J.A. Last, N. Sahai, Role of oxide surface chemistry and phospholipid phase on adsorption and self-assembly: isotherms and atomic force microscopy, J. Phys. Chem. C 113 (2009) 2187–2196.
[21] K. Ariga, Silica-supported biomimetic membranes, Chem. Rec. 3 (2004) 297–307.
[22] S. Mornet, O. Lambert, E. Duguet, A. Brisson, The formation of supported lipid bilayers on silica nanoparticles revealed by cryoelectron microscopy, Nano Lett. 5 (2005) 281–285.
[23] M.M. Baksh, M. Jaros, J.T. Groves, Detection of molecular interactions at membrane surfaces through colloid phase transitions, Nature 427 (2004) 139–141.
[24] R.W. Davis, A. Flores, T.A. Barrick, J.M. Cox, S.M. Brozik, G.P. Lopez, J.A. Brozik, Nanoporous microbead supported bilayers: stability, physical characterization, and incorporation of functional transmembrane proteins, Langmuir 23 (2007) 3864–3872.
[25] K. Suzuki, H. Masuhara, Groove-spanning behavior of lipid membranes on microfabricated silicon substrates, Langmuir 21 (2005) 6487–6494.
[26] T. Buranda, J. Huang, G.V. Ramarao, L.K. Ista, R.S. Larson, T.L. Ward, L.A. Sklar, G.P. Lopez, Biomimetic molecular assemblies on glass and mesoporous silica microbeads for biotechnology, Langmuir 19 (2003) 1654–1663.
[27] A.M. Brozell, M.A. Muha, B. Sanii, A.N. Parikh, A class of supported membranes: formation of fluid phospholipid bilayers on photonic band gap colloidal crystals, J. Am. Chem. Soc. 128 (2006) 62–63.
[28] E.E. Ross, M.J. Wirth, Silica colloidal crystals as three-dimensional scaffolds for supported lipid films, Langmuir 24 (2008) 1629–1634.
[29] D.A. Doshi, A.M. Dattelbaum, E.B. Watkins, C.J. Brinker, B.I. Swanson, A.P. Shreve, A.N. Parikh, J. Majewski, Neutron reflectivity study of lipid membranes assembled on ordered nanocomposite and nanoporous silica thin films, Langmuir 21 (2005) 2865–2870.
[30] K.C. Weng, J.J.R. Stalgren, D.J. Duval, S.H. Risbud, C.W. Frank, Fluid biomembranes supported on nanoporous aerogel/xerogel substrates, Langmuir 20 (2004) 7232–7239.
[31] K.C. Weng, J.J.R. Stalgren, S.H. Risbud, C.W. Frank, Planar bilayer lipid membranes supported on mesoporous aerogels, xerogels, and Vycor((R)) glass: an epifluorescence microscopy study, J. Non-Cryst. Solids 350 (2004) 46–53.
[32] C.J. Brinker, Sol–Gel Processing of Silica., The Colloid Chemistry of Silica, vol. 234, American Chemical Society, Washington, DC, 1994, pp. 361–402.
[33] Q. Liu, J. Zhang, Q.J. Liu, Z.Q. Zhu, J. Chen, Sol–gel synthesis and characterization of silica film with two opposite structures: nano-porous and protuberant, Mater. Chem. Phys. 114 (2009) 309–312.
[34] G.M. Wu, J. Wang, J. Shen, T.H. Yang, Q.Y. Zhang, B. Zhou, Z.H. Deng, B. Fan, D.P. Zhou, F.H. Zhang, A new method to control nano-porous structure of sol–gel-derived silica films and their properties, Mater. Res. Bull. 36 (2001) 2127–2139.
[35] K. Jacobson, C. Dietrich, Looking at lipid rafts? Trends Cell Biol. 9 (1999) 87–91.
[36] K. Simons, E. Ikonen, Functional rafts in cell membranes, Nature 387 (1997) 569–572.
[37] A.W. Szmodis, C.D. Blanchette, A.A. Levchenko, A. Navrotsky, M.L. Longo, C.A. Orme, A.N. Parikh, Direct visualization of phase transition dynamics in binary supported phospholipid bilayers using imaging ellipsometry, Soft Matter 4 (2008) 1161–1164.
[38] E.I. Goksu, J.M. Vanegas, C.D. Blanchette, W.C. Lin, M.L. Longo, AFM for structure and dynamics of biomembranes, Biochim. Biophys. Acta, Biomembr. 1788 (2009) 254–266.
[39] E.I. Goksu, B.A. Nellis, W.-C. Lin, J.H. Satcher, J.T. Groves, S.H. Risbud, M.L. Longo, Effect of support corrugation on silica-xerogel supported phase-separated lipid bilayers, Langmuir 25 (2009) 3713–3717.
[40] M.I. Hoopes, M. Deserno, M.L. Longo, R. Faller, Coarse-grained modeling of interactions of lipid bilayers with supports, J. Chem. Phys. 129 (2008) 175102.
[41] K.S.W. Sing, D.H. Everett, R.A.W. Haul, L. Moscou, R.A. Pierotti, J. Rouquerol, T. Siemieniewska, Reporting physisorption data for gas solid systems with special reference to the determination of surface-area and porosity (Recommendations 1984), Pure Appl. Chem. 57 (1985) 603–619.
[42] M. Cantin, M. Casse, L. Koch, R. Jouan, P. Mestreau, D. Roussel, F. Bonnin, J. Moutel, S.J. Teichner, Silica aerogels used as Cherenkov radiators, Nucl. Instrum. Methods 118 (1974) 177–182.
[43] T.F. Baumann, A.E. Gash, G.A. Fox, J.H. Satcher, L.W. Hrubesh, Handbook of Porous Solids, Wiley-VCH Weinheim, 2002.
[44] J. Zarzycki, Structural Aspects of Sol–Gel Synthesis, 1990, pp. 110–118.
[45] D.L. Meixner, P.N. Dyer, Influence of sol–gel synthesis parameters on the microstructure of particulate silica xerogels. J. Sol–Gel Sci. Technol. 14 (1999) 223.
[46] J. Sefcik, A.V. McCormick, Kinetic and thermodynamic issues in the early stages of sol–gel processes using silicon alkoxides, Catal. Today 35 (1997) 205–223.
[47] B.N. Nair, W.J. Elferink, K. Keizer, H. Verweij, Sol–gel synthesis and characterization of microporous silica membranes. 1. SAXS study on the growth of polymeric structures, J. Colloid Interface Sci. 178 (1996) 565–570.
[48] W.J. Elferink, B.N. Nair, R.M. DeVos, K. Keizer, H. Verweij, Sol–gel synthesis and characterization of microporous silica membranes. 2. Tailor-making porosity, J. Colloid Interface Sci. 180 (1996) 127–134.
[49] K.J. Seu, A.P. Pandey, F. Haque, E.A. Proctor, A.E. Ribbe, J.S. Hovis, Effect of surface treatment on diffusion and domain formation in supported lipid bilayers, Biophys. J. 92 (2007) 2445–2450.
[50] M. Rodahl, F. Hook, B. Kasemo, QCM operation in liquids: an explanation of measured variations in frequency and Q factor with liquid conductivity, Anal. Chem. 68 (1996) 2219–2227.
[51] P.F. Devaux, Static and dynamic lipid asymmetry in cell-membranes, Biochemistry 30 (1991) 1163–1173.
[52] J.B. Helms, C. Zurzolo, Lipids as targeting signals: lipid rafts and intracellular trafficking, Traffic 5 (2004) 247–254.
[53] P. Keller, D. Toomre, E. Diaz, J. White, K. Simons, Multicolour imaging of post-Golgi sorting and trafficking in live cells, Nat. Cell Biol. 3 (2001) 140–149.
[54] K.C. Weng, J.J.R. Stalgren, S.H. Risbud, C.W. Frank, Planar Bilayer Lipid Membranes Supported on Mesoporous Aerogels, Xerogels, and Vycor((R)) Glass: An Epifluorescence Microscopy Study, Elsevier Science Bv, 2004, pp. 46–53.
[55] L. Guo, J.Y. Har, J. Sankaran, Y.M. Hong, B. Kannan, T. Wohland, Molecular diffusion measurement in lipid bilayers over wide concentration ranges: a comparative study, ChemPhysChem 9 (2008) 721–728.
[56] Y. Roiter, M. Ornatska, A.R. Rammohan, J. Balakrishnan, D.R. Heine, S. Minko, Interaction of nanoparticles with lipid membrane, Nano Lett. 8 (2008) 941–944.
[57] U. Seifert, K. Berndl, R. Lipowsky, Shape transformations of vesicles—phase-diagram for spontaneous-curvature and bilayer-coupling models, Phys. Rev. A 44 (1991) 1182–1202.
[58] S.A. Safran, P. Pincus, D. Andelman, Theory of spontaneous vesicle formation in surfactant mixtures, Science 248 (1990) 354–356.
[59] P.S. Swain, D. Andelman, Supported membranes on chemically structured and rough surfaces, Phys. Rev. E 63 (2001) 12.
[60] A. Tian, T. Baumgart, Sorting of lipids and proteins in membrane curvature gradients, Biophys. J. 96 (2009) 2676–2688.
[61] B. Sanii, A.M. Smith, R. Butti, A.M. Brozell, A.N. Parikh, Bending membranes on demand: fluid phospholipid bilayers on topographically deformable substrates, Nano Lett. 8 (2008) 866–871.
[62] J.H. Werner, G.A. Montaǹo, A.L. Garcia, N.A. Zurek, E.A. Akhadov, G.P. Lopez, A.P. Shreve, Formation and dynamics of supported phospholipid membranes on a periodic nanotextured substrate, Langmuir 25 (2009) 2986–2993.
[63] R. Parthasarathy, C.h. Yu, J.T. Groves, Curvature-modulated phase separation in lipid bilayer membranes, Langmuir 22 (2006) 5095–5099.

[64] P.D. Thomas, M.J. Poznansky, Effect of surface curvature on the rate of cholesterol transfer between lipid vesicles, Biochem. J. 254 (1988) 155–160.
[65] W.C. Wang, L. Yang, H.W. Huang, Evidence of cholesterol accumulated in high curvature regions: implication to the curvature elastic energy for lipid mixtures, Biophys. J. 92 (2007) 2819–2830.
[66] S. Ahmed, S.L. Wunder, Effect of high surface curvature on the main phase transition of supported phospholipid bilayers on SiO2 nanoparticles, Langmuir 25 (2009) 3682–3691.
[67] K.E. Eigenberg, S.I. Chan, The effect of surface curvature on the headgroup structure and phase-transition properties of phospholipid-bilayer vesicles, Biochim. Biophys. Acta 599 (1980) 330–335.
[68] A.N. Dickey, R. Faller, Molecular modeling of biomembranes: a how-to approach, in: T. Jue (Ed.), Handbook of Modern Biophysics, Vol. 3: Biomedical Applications in Biophysics Springer, 2009, pp. 35-58 (in press).
[69] J.L. MacCallum, D.P. Tieleman, Interactions between small molecules and lipid bilayers, Curr. Top. Membr. 60 (2008) 227–256.
[70] M.I. Hoopes, C. Xing, R. Faller, Multiscale modeling of supported lipid bilayers, in: T. Jue, R. Faller, M.L. Longo, S.H. Risbud (Eds.), Handbook in Modern Biophysics 2: Biomembrane Frontiers: Nanostructures, Models, and the Design of Life Springer, Humana, Totowa, NJ, 2009, pp. 101–120.
[71] M. Roark, S.E. Feller, Structure and dynamics of a fluid phase bilayer on a solid support as observed by a molecular dynamics computer simulation, Langmuir 24 (2008) 12469–12473.
[72] D.R. Heine, A.R. Rammohan, J. Balakrishnan, Atomistic simulations of the interaction between lipid bilayers and substrates, Mol. Simul. 33 (2007) 391–397.
[73] M. Tarek, K. Tu, M.L. Klein, D.J. Tobias, Molecular dynamics simulations of supported phospholipid/alkanethiol bilayers on a gold(111) surface, Biophys. J. 77 (1999) 964–972.
[74] A. Pertsin, D. Platonov, M. Grunze, Computer simulation of short-range repulsion between supported phospholipid membranes, Biointerphases 1 (2006) 40–49.
[75] S.V. Bennun, M.I. Hoopes, C. Xing, R. Faller, Coarse-grained modeling of lipids, Chem. Phys. Lipids (2009) 59–66.
[76] S.J. Marrink, A.H. de Vries, A.E. Mark, Coarse grained model for semi-quantitative lipid simulation, J. Phys. Chem. B 108 (2004) 750–760.
[77] S.J. Marrink, H.J. Risselada, S. Yefimov, D.P. Tieleman, A.H. de Vries, The MARTINI force field: coarse grained model for biomolecular simulations, J. Phys. Chem. B. 111 (2007) 7812–7824.
[78] I.R. Cooke, K. Kremer, M. Deserno, Tunable generic model for fluid bilayer membranes, Phys. Rev. E 72 (2005) 011506.